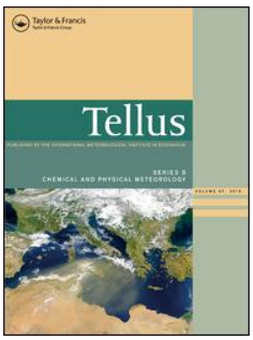

Tellus B: Chemical and Physical Meteorology

ISSN: (Print) 1600-0889 (Online) Journal homepage: https://www.tandfonline.com/loi/zelb20

Orisam-TM4 : a new global sectional multi-component aerosol model including SOA formation - Focus on carbonaceous BC and OC aerosols

B. Guillaume, C. Liousse, R. Rosset, H. Cachier, P. Van Velthoven, B. Bessagnet & N. Poisson

To cite this article: B. Guillaume, C. Liousse, R. Rosset, H. Cachier, P. Van Velthoven, B. Bessagnet & N. Poisson (2007) Orisam-TM4 : a new global sectional multi-component aerosol model including SOA formation - Focus on carbonaceous BC and OC aerosols, Tellus B: Chemical and Physical Meteorology, 59:2, 283-302

To link to this article: https://doi.org/10.1111/j.1600-0889.2007.00246.x

Tellus (2007), 59B, 283–302
Printed in Singapore. All rights reserved

TELLUS

ORISAM-TM4 : a new global sectional multi-component aerosol model including SOA formation - Focus on carbonaceous BC and OC aerosols

By B. GUILLAUME[1]*, C. LIOUSSE[1], R. ROSSET[1], H. CACHIER[2], P. VAN VELTHOVEN[3], B. BESSAGNET[4] and N. POISSON[5], [1]*Laboratoire d'Aérologie – TOULOUSE, France;* [2]*Laboratoire des Sciences du Climat et de l'Environnement – GIF –SUR-YVETTE, France;* [3]*Royal Netherlands Meteorological Institute – Section of Atmospheric Composition – DE BILT, The Netherlands;* [4]*INERIS – VERNEUIL-EN-HALATTE, France;* [5]*ADEME – rue Louis Vicat – PARIS, France*

(Manuscript received 4 January 2006; in final form 17 November 2006)

ABSTRACT

Few global aerosol models deal with size differentiated inorganic/organic particles. Among them, still fewer ones explicitly treat secondary organic aerosol (SOA) formation. In this context, we have coupled the global chemistry-transport model (CTM) TM4 (Van Velthoven et al., 1996) and the aerosol sectional model ORISAM (ORganic and Inorganic Sectional Aerosol Model, Bessagnet et al., 2002). This new aerosol model ORISAM-TM4 can accommodate aerosol size distributions with a variable number of diameter sections (bins) between 0.04 μm and over 10 μm and detailed organic/inorganic chemistry coupled with optional gas schemes. Two model versions are presented: a tracer version and a fully detailed eight-bin version with SOA formation. Focus is made on carbonaceous BC (black carbon) and OC (organic carbon) aerosols. First, significant developments both in ORISAM and in TM4 are discussed in line with the incorporation of updated emission inventories of BC and primary OC (OCp). Then, general comparisons are made between simulated BC and OC concentrations in air and precipitation against worldwide measurements. Also for BC, sensitivity tests using different updated fossil fuel emission inventories are focused over Europe, where emission controls make great strides. The tracer version appears generally satisfactory for BC mostly at background and remote sites, but not for total OC. For this latter, quite significant improvements result from the incorporation of SOA formation in ORISAM-TM4, instead of estimating OC as being simply proportional to OCp, as done in most existing models. Conclusions and prospects are then given.

1. Introduction

Various studies have highlighted the complex interactions between climate and aerosol microphysical, chemical and radiative properties, particularly its carbonaceous components (Penner et al., 1992; Liousse et al., 1996; Heintzenberg et al., 1997; Cachier, 1998; Cooke et al., 1999). Recently, it has been suggested that, due to complex aerosol absorption/diffusion radiative characteristics and brief atmospheric residence times, reduction policies targetting at aerosol emissions could be more rapidly effective against climate change than greenhouse gases (Jacobson, 2002; Bond and Sun, 2005). However, most global aerosol models only poorly grasp aerosol complexity.

A few requirements on aerosol modelling emerge from recent papers, basically about size distributions and chemical composition, sometimes with a hierarchy between them (Dusek et al., 2006). Size distributions are crucial in detailed microphysical processes (e.g. condensation, coagulation, ageing, etc.), for radiative and hygroscopic properties (growth characteristics and aerosol-cloud interactions), also for radiative effects. As for their inorganic and organic chemical composition, aerosol emissions, gas–particle (GP) interactions and evolving external/internal mixing at different ageing stages are also essential for aerosol hygroscopic and radiative properties. In the following, some present global aerosol models are briefly reviewed.

Some of these models simulate the evolution of bulk aerosol mass with no size differentiation. Among these models, aerosols are treated either as external mixtures (multicomponent aerosols in Lohmann et al. (1999) or only BC and OC in Cooke et al. (1999)) or as internal mixtures with prescribed constant ratios between individual components (Haywood et al. (1997) for sulfates and BC). In these models, such major aerosol outputs as radiative effects, quite sensitive to aerosol size distributions and to aerosol mixing state (internal/external), are poorly evaluated.

*Corresponding author.
e-mail : guib@aero.obs-mip.fr
DOI: 10.1111/j.1600-0889.2006.00246.x

Evolving size distributions were also introduced for single component aerosols (dust in Tegen and Lacis, 1996, sulfates in Chin et al., 1996) as well as for multi-component ones (inorganic species (sulfates, nitrates, ammonia) in Adams et al. (1999), Jacobson (2001a) and Adams and Seinfeld (2002), inorganics and dust in Rodriguez and Dabdub (2004) and Spracklen et al. (2005)). At this stage, few global aerosol models combine size-differentiated microphysics with inorganic/organic chemical composition without secondary organic aerosol (SOA) formation, either using multimodal (M7 in Vignati et al., 2004) or sectional approaches (ECHAM-HAM in Stier et al., 2004; IMPACT in Liu et al., 2005). In such models, carbonaceous aerosols were treated as tracer species, though the traceable part of OC (OCp) is only about or below 50% of the total OC mass, the rest being of secondary origin (Cooke et al., 1999; Heald et al., 2005). Modelling SOA chemical formation is still at a beginning stage, only about 10% of SOA mass having been experimentally identified. One recent global model with SOA formation is by Tsigaridis and Kanakidou (2003), though with no specification of size distributions.

Some mesoscale/regional aerosol models incorporate SOA formation and size distributions (e.g. Bessagnet et al., 2002; Cousin et al., 2005; Pun et al., 2006). Here such an approach has been extended to the global scale. For this purpose, after due adaptations, we have implemented the aerosol sectional model ORganic and Inorganic Sectional Aerosol Model (ORISAM) (Bessagnet et al., 2002) within the TM4 global chemistry transport model (Van Velthoven and Kelder, 1996). This new aerosol model ORISAM-TM4 is apt to accommodate size-differentiated chemistry in a selectable number of bins (e.g. between 0.04 μm and over 10 μm) and optional gas phase chemistry schemes. Though the model also provides other (inorganic) aerosol components, focus is here on the concentrations of carbonaceous aerosol components BC and OC. Two versions of ORISAM-TM4 were constructed, namely a tracer version suitable for BC and a full aerosol version including SOA formation. Modelled BC concentrations from the tracer version has been tested against BC and OC concentrations measured in air and precipitation at a worldwide selected set of stations, spanning a wide range of climatic environments. Also, as a prerequisite to these tests, a detailed description of new BC and OCp emission inventories (Liousse et al., 2004; Junker and Liousse, 2006) is presented and with special interest on Europe where more and more stringent anthropic emission controls, mainly on fossil fuels, are applied, with increasing needs to evaluate their impacts. Therefore, tests have been made on such different available European updated emission inventories which differently incorporate these anti-pollution norms (Schaap et al., 2004; Guillaume and Liousse, 2006). These emission inventories, embedded into global ones, were then processed in the BC tracer version before modelled concentrations were evaluated against a set of concentrations measured at European rural sites. Finally, OC concentrations modelled with the full aerosol version are tested against a selected set of worldwide measurements in quite different climatic situations, followed by discussion on the improvements brought by including both SOA formation and size distributions in OC modelling.

2. ORISAM aerosol modelling in TM4

The sectional inorganic/organic aerosol model ORISAM (Warren and Seinfeld, 1985; Bessagnet et al., 2002; Cousin et al., 2005; Liousse et al., 2005) has been implemented within the global chemistry-transport model (CTM) TM4 (Dentener and Crutzen, 1994; Van Velthoven and Kelder, 1996; Jeuken et al., 2001). The salient features of both models are first briefly described. Then, the adaptations made in ORISAM and in TM4 for implementation purpose are presented.

2.1. The basic TM4 chemistry-transport host model

The basic TM4, hereafter described, refers to TM4 before any modification for implementation purpose. TM4 is driven by ERA40 reanalyzed meteorological fields from the European Meteorological Centre (ECMWF) (http://www.ecmwf.int/research/era/) and for present fields by daily operational ECMWF analyses, both preprocessed for use in TM4 by KNMI (http://www.knmi.nl/∼velthove/tm.html). Transport equations are solved for mass mixing ratios of 31 gaseous species using Russell and Lerner's (1981) advection scheme at $3^\circ \times 2^\circ$ horizontal resolution and 31 hybrid sigma-pressure vertical levels. Tropospheric gas phase chemistry is a modified version of CBM-IV (Houweling et al., 1998) solved by an Euler-backward iterative method (Hertel et al., 1993). Bulk aqueous-phase chemistry of cloud droplets is treated after Jeuken et al. (2001): SO_2 dissolution results in the formation of HSO_3^-, SO_3^{2-} and sulfates whereas NH_3 dissolution gives NH_4^+ ions. Overall sulphate to ammonia ratios in the TM4 particulate phase are computed using only bulk microphysics.

The dry deposition scheme is after Ganzeveld et al. (1998). Gas dry deposition obeys a resistance scheme (Wesely and Hicks, 2000) applied to the vegetation types of Olson et al. (1983).

The TM4 wet deposition scheme including additional features introduced in the new ORISAM-TM4 version will be further discussed in Section 2.3.

Gaseous emissions in TM4 comprise NOx, NH_3, SO_2, CO and CH_4 from anthropogenic and biogenic sources for the year 1995, using the EDGAR 3.2 database (Olivier et al., 1999: http://arch.rivm.nl/env/int/coredata/edgar/index.html), together with NMHC emissions from the POET database (Olivier et al., 2003), non-eruptive volcanic SO_2 emissions from GEIA, NOx due to aviation (ANCAT, 1998), lightning-NOx and online calculated DMS emissions. An alternative to CH_4 emissions in TM4 is to use previously assimilated CH_4 surface concentrations. At the upper boundary (10 hPa), ozone climatology, CH_4

stratospheric fluxes and CH_4 mixing ratios are fixed with prescribed HNO_3/O_3 ratios from satellite UARS CLAES data.

2.2. The aerosol model ORISAM

A detailed description of the ORISAM can be found in Bessagnet et al. (2002), Cousin et al. (2005) and Liousse et al. (2005). Both aerosol mass and number size distributions evolve in a sectional framework (bins) subject to microphysical processes (nucleation, condensation, absorption, coagulation, sedimentation, deposition) and chemical transformations, including SOA formation. Here, when aerosol size distributions are mentioned (with corresponding median diameter m and dispersion coefficient σ), they all refer to mass distributions and not to number distributions.

Aerosol microphysics models most often use modal (Binkowski and Shankar, 1995) or sectional (bins) approaches (Gelbard et al., 1980). In ORISAM, the sectional approach has been selected due to its potential for detailed aerosol microphysical processes without a priori assumptions on size distributions. Typically, the aerosol size range in ORISAM varies between 0.04 nm and 10 μm, with a selectable number of adjacent bins possibly having different initial chemical compositions, then each bin evolving separately according to the processes hereafter.

Nucleation is after Kulmala et al. (1998) and coagulation as in Gelbard et al. (1980). Nitrate heterogeneous chemistry (Jacob, 2000) is also implemented. GP partitioning for inorganics is solved using ISORROPIA (Nenes et al., 1998), while empirical partitioning coefficients Kp are used for organics (Odum et al., 1996).

2.3. Implementation of ORISAM in TM4 and due adaptations

To implement ORISAM in TM4, several modifications and improvements had to be brought to both models. The basic TM4 initial vertical resolution of 31 vertical levels was reduced for cheaper computational tests with ORISAM-TM4. A nine-level tracer version is currently used, when no further precision is necessary. A 19-level version has been tested here in some cases, when enough resolution in the boundary layer is necessary for improving BC concentration modelling. As for the full aerosol version, a nine-level version is commonly used, which can accommodate a large number of bins (e.g. up to 20). In the tests reported here, current use is made of a nine-level, eight-bin version. These eight bins are in the range 0.04–10 μm with average geometrical diameters, respectively, equal to 0.06, 0.11, 0.22, 0.45, 0.89, 1.78, 3.05 and 7.08 μm. The major processes effectively activated are examined now.

2.3.1. SOA formation. SOA formation requires gas-phase chemistry schemes apt to effectively treat major volatile, semi-volatile and non-volatile organics at successive oxidation stages. SOA formation in ORISAM is based on VOC-lumping and empirical aerosol yields. The chemical scheme in the basic TM4 was mainly designed for O_3 chemistry, while VOC chemistry required for SOA formation is quite more complex. Hence, the Houweling et al.'s (1998) basic CBM-IV scheme in TM4 had to be deeply modified to account for SOA formation. This was done by inclunding TX (toluene, xylenes) and terpenes (mainly alpha- and beta-pinenes), in terms of emissions (Olivier et al., 2003) and chemical pathways (Hertel et al., 1997) including temperature-dependent oxidation rates (cf. Table 1). Then, aerosol yields (Tsigaridis and Kanakidou, 2003) were applied to form condensable species (Table 1), either as SOAA (anthropogenic SOA) or SOAB (biogenic SOA).

Though mesoscale/regional studies (Pandis et al., 1992; Bessagnet et al., 2004; Cousin et al., 2005) have put forward the importance of long-chained alkanes/alkenes in SOA formation, especially in urban/industrial areas and other recent studies have insisted upon isoprene (Ervens et al., 2004; Lim et al., 2005) and benzene (Martin-Reviejo and Wirtz, 2005) as SOA precursors, these species were not retained here due to still large uncertainties on these precursors.

2.3.2. Microphysical processes. GP mass transfer of condensable species occurs through adsorption at the particle surface or absorption within bulk particles, with the diffusion time scales increasing with aerosol diameters. Thus, for fine particles, condensable species rapidly reach GP equilibria whereas such equilibria, are longer to be reached for coarse particles (Wexler and Seinfeld, 1990).

In ORISAM, the condensation equations (absorption/adsorption) are solved in time according to a 'full-dynamical approach' (Bessagnet et al., 2002; Cousin et al., 2005), using a classical ODE solver (0D version) or cheaper solvers, QSSA or TWOSTEP in 3D versions. With the large time steps required in global models for long-term integrations, the 'full-dynamical solution' becomes unstable with increasing oscillations. Recently, Jacobson (2005) has proposed an approach for the 'full-dynamical' solution by putting an additional constraint on the pH of particles. However, such a solution is not yet available for organics. Consequently, another approach, 'the full-equilibrium solution' is used, considering the long time step (1800s) in ORISAM-TM4. This solution assumes equilibria to be reached for all bins after each time step, though with some inherent overestimation for large (supermicron) particles, which could reach equilibria only after about 1 hr. In this full-equilibrium approach, the condensed mass is transferred to bins according to weights derived from condensation factors (Zhang et al., 2004). Tests with ORISAM-TM4 have shown that this solution is valid for inorganics whereas for organics, the overestimation is too important due to stronger non-linear effects in the condensation equations for organics than for inorganics. Hence, we have imposed the additional constraint of a total condensation for organics, resulting in stable valid solutions for the whole inorganics/organics system. In the next future, a 'hybrid approach' combining equilibria for small

Table 1. Additional reactions in ORISAM-TM4 to Houweling's CBM4 modified scheme

Anthropogenic and biogenic	Rate constants	Aerosol yields
Reactions with new products[a]	(in cm^3/molec/s)[a]	(molec/molec)[b]
TOL + OH -> a2 [a] **SOAA** + ...	$1.81.10^{-12}$ exp(−355./T)	a2 = 0.07
XYL+OH -> a3 [a] **SOAA** + ...	$7.3.10^{-12}$ exp(−355./T)	a3 = 0.05
TERP + OH -> b1 [a] **SOAB** + ...	$1.21.10^{-11}$ exp(−444./T)	b1 = 0.12

[a]Hertel et al. (1997).
[b]Tsigaridis and Kanakidou (2003).

particles (typical diameters below 2.5 μm) and dynamical transfer for coarser ones (Pilinis et al., 2000) will be tested.

Due to such GP transfer complexity in the full inorganics/organics system (Zhang et al., 2004), separate equilibria resolutions for 'organics' and for 'water/inorganics' were kept in ORISAM-TM4, at this stage.

Nucleation and coagulation were inserted, but not activated (Wexler et al., 1994) in the preliminary tests reported here.

2.3.3. Parametrization of wet deposition. Detailed treatment of the interactions between clouds and aerosols is beyond our present scope, though several studies have recently explored the impact of such complex processes in global models (e.g. Nenes and Seinfeld, 2003; Ming et al., 2006). Consequently, ORISAM-TM4 includes only a rough aqueous-phase chemistry, based on Jeuken et al. (2001).

2.3.3.1. Aerosol activated fraction. Aerosol activation to CCN and cloud droplets is dependent on cloud vertical velocities, supersaturations, aerosol size distributions and chemical composition. Here, we use a simplified empirical/mechanistic parameterization of CCN activation suitable for sectional models (Zhang et al., 2004), considering two types of parametrizations : a detailed parametrization for bin numbers over 6, against a coarse one for bin numbers between 2 and 5 (Table 2). In the tracer version, particles are in a unique accumulation mode (0.6 μm), the activated aerosol mass fraction being fixed to 80%.

Table 2. Parametrization of activated aerosol mass fractions (Zhang et al., 2004)

Particle size range (mass-distribution diameters in μm)	Activated mass fraction (in%)
Case 1: Over 6 bins in the range 0.04–10 μm	
Dp> 0.35μm	100
0.1μm<Dp≤0.35μm	50
Dp≤0.1μm	0
Case 2 (2 to 5 bins)	
Dp>2.5μm	100
Dp ≤ 2.5μm	80
Case 3 (tracer version)	
Dp ≈ 0.6 μm	80

Sulphate particles formed in cloud droplets (cf. Section 2.1) and only distributed in the activated aerosol bins are proportional to aerosol number concentrations (Rodriguez and Dabdub, 2004). For carbonaceous aerosols, only hydrophilic components are activated as cloud droplets.

2.3.3.2. Particle hygroscopicity and ageing. After emission partitioning into hydrophobic and hydrophilic BC and OCp fractions, these latter evolve through absorption, condensation and coagulation (Riemer et al., 2004), as well as through surface reactions. The link between these diverse ageing processes and particle hygroscopicity remains a main subject of research (Tsigaridis and Kanakidou, 2003; Liu et al., 2005; Poeschl et al., 2001): for carbonaceous aerosols, no consensual corresponding parametrizations are available. Therefore, even if ORISAM-TM4 provides an estimate of the condensed mass, still ongoing works aims at relating this latter to the hydrophobic/hydrophilic transformation processes. An alternative approach used here is to introduce a constant turn-over time (Cooke et al., 1999) to grossly parameterize ageing of BC and primary OC particles between their sources (there mainly hydrophobic) and remote sites (more hydrophilic states). The empirical 1-d constant of Cooke et al. (1999) was kept in ORISAM-TM4.

Concerning SOA hygroscopicity, both SOAA and SOAB components are considered 100% hydrophilic, certainly overestimating SOA wet removal. Next improvements will involve mechanistic VOC organic gas schemes, specifically considering both hydrophobic and hydrophilic condensable species (Pun et al., 2003).

2.3.3.3. In-cloud aerosol precipitation scavenging. In-cloud aerosol precipitation scavenging is modelled using an implicit approach based on precipitation data issued from ERA-40 reanalyses, with a distinction between convective and layer clouds (Jeuken et al., 2001). For liquid and ice layer clouds, removal rates are proportional to precipitation formation rates, the vertical profiles of which are calculated online (Sundquist et al., 1989; Heymsfield and Donner, 1990), with surface rainout (also from ERA-40 reanalyses) being an additional control variable. For convective clouds, removal rates are assumed proportional to convective updrafts (Jeuken et al., 2001) with 50% effective scavenging in shallow convection against 100% in deep convection. Particles not scavenged by these processes are assumed totally released in the atmosphere after evaporation.

Convective scavenging thus parametrized and tested for BC wet deposition in the Tropics appeared largely overestimated in ORISAM-TM4, with simulated values higher by a factor of 10. So, the previous first-order convective scavenging scheme in the TM2z model (Guelle et al., 1998), has been reintroduced into ORISAM-TM4, then leading to significant improvements in BC wet deposition in the Tropics.

2.3.3.4. Below-cloud aerosol precipitation scavenging. Below-cloud aerosol scavenging is parameterized via the determination of collection efficiency functions (Slinn, 1977), which are bivariate functions of both aerosol and raindrop diameters. They simplify as monovariate functions only dependent on aerosol diameters (Slinn, 1977), with assumed lognormal rain drop distributions. For fine particles, this function smoothly varies with aerosol diameters. Therefore, in the tracer version with particles of mass diameters below 0.6 μm, a reference washout coefficient of 0.05 mm^{-1} was adopted (Dana and Hales, 1976).

2.3.4. Parametrization of dry deposition and sedimentation processes. Aerosol dry deposition parametrization in the TM4 dry deposition scheme has been already mentioned, with particle deposition velocities after Seinfeld and Pandis (1998). Dry deposition velocities are in the range 0.1–1 cm s^{-1}, in agreement with current observations.

Gravitational settling applied to all model levels, was expressed as the time for particles to fall 1 km, ranging from 228 yr for 0.02 μm diameter particles to 3.6 d for 10 μm ones (Jacobson, 1999).

3. Emission inventories of carbonaceous aerosols

Our main focus here with ORISAM-TM4 being on carbonaceous aerosols, strong prerequisites on BC and OCp emissions are needed for OC modelling. These emissions are still hampered by severe uncertainties (Bond et al., 2004) resulting from large differences in the choice of emission factors. In the following, updates of BC and OCp emission inventories implemented in ORISAM-TM4 are detailed source-by-source.

3.1. Fossil fuel sources

Two major different approaches for deriving fossil fuel BC and OCp emission inventories are currently available, Cooke et al. (1999) and Bond et al. (2004), the main difference being in technology differentiations. Thus, Bond et al. consider for each fossil fuel a detailed list of combustion technologies with associated EF, while in Cooke et al., for each fuel, two parameters characterize the emissions: the sector of activity (domestic, industrial, traffic) and the national level of development based on GNB (with three classes: developed, semi-developed and developing countries).

For developed countries mostly and since about 1990, new technologies and new emission controls have made great strides, though not fully effectively applied. This, even stronger, applies to semi-developed and developing countries. Estimation of the part of uncontrolled emissions is at the origin of the largest differences between the two approaches above, with higher estimated emissions for the major fuels (coal, diesel, peat, lignite and coke) in Cooke et al. As for controlled emissions, more account given in Bond et al. than in Cooke et al.

Clearly, harmonization between these two inventory types is required and is in progress, resulting in recent emission updatings in Cooke et al. at the global (Junker and Liousse, 2006) and at European scale (Guillaume and Liousse, 2006). At the global scale, this harmonization consists for instance in revised EF for traffic diesel, now being 5 g kg^{-1} instead of 10 g /kg^{-1} for developing countries. Concerning Europe, this harmonization consists to introduce new technologies and emission controls, which are rapidly evolving in Europe, while keeping high EF values for uncontrolled emissions.

In the global simulations to follow, the new updated global inventory is used for the year 1997 while for Europe, particular sensitivity tests have been performed upon the different available European BC emission inventories through processing within the ORISAM-TM4 tracer version. For this purpose, the four following scenarios have been tested, listed from the least to the most uncontrolled emission inventories:

(1) S1 scenario, using Schaap et al. (2004) with BC emission inventory for the year 1995 derived from Bond et al.

(2) S2 scenario, using the 'low scenario' in Guillaume and Liousse (2006), with BC emission inventory based on Cooke et al. but enhanced using both new technologies and emission controls for the year 1995 too.

(3) S3 scenario, using the 'high scenario' in Guillaume and Liousse (2006), similar to S2 though without any emission controls applied.

(4) S4 scenario, using the Junker and Liousse (2006) BC emission inventory for the year 1997.

Emission inventories in S1, S2 and S3 are built with 25 km $\times$ 25 km resolution against $1^\circ \times 1^\circ$ resolution for S4. They are then extrapolated to ORISAM-TM4 resolution and embedded in the global emission inventory of Junker and Liousse (2006).

Results of these sensitivity tests are reported in Section 4.2.3, while S2 (the 'low scenario') is hereafter used as the reference scenario for all simulations.

3.2. Biomass burning

Updated biomass burning BC and OCp emissions from Liousse et al. (2004) were selected for ORISAM-TM4 simulations since two main differences on EF appear when compared to previous inventories. The first one is on the development of OCp emissions instead of total OC, OCp emissions being more suitable here since ORISAM-TM4 explicitly treats SOA formation with ensuing variable OCp/OC ratios. The second difference lies in OCp emission factors with separate values from aircraft and ground measurements. Aircraft measurements incorporate

aged particles with SOA, less the case for ground measurements, mostly dealing with fresh OCp emissions (Liousse et al., 2004). Since using ORISAM-TM4 for SOA formation, OCp ground emissions were used here.

3.3. Other sources

Other emissions incorporated into ORISAM-TM4 are domestic (fuelwood, charcoal, animal wastes, etc.) and agricultural biofuel combustion ones from Liousse et al. (1996).

3.4. Further characteristics of BC and OCp emission inventories

Further characteristics of these emissions in ORISAM-TM4 are described now, namely their seasonality, injection heights and initial size distributions, listed in Table 3 for the first two ones.

Biofuel domestic combustion (fuelwood, charcoal and charcoal making) as well as savanna/forest/agricultural fires follow an imposed seasonal variation (Liousse et al., 1996). Fossil fuel combustion (industrial, domestic other than biofuels and road traffic combustion) are not subject to seasonal variations, except domestic use of liquid fuels (diesel, heavy fuels) with the same seasonality as domestic biofuel combustion. Resulting emissions for August 2002 and January 2003 are displayed in Fig. 1, showing quite different patterns in particular over the African continent.

Emission injection heights displayed in Table 3 refer to the highest injection altitudes (n). Additionally, the vertical distribution of injected emissions between the ground and these n-levels is as follows: 50% are injected at level n, 25% at level n–1,etc.. Levels 1 and 2 are attributed both half the rest of emissions (Lavoue et al., 2000).

The size distributions of emitted BC and OC particles, relying on measurements during the Escompte 2001 campaign (Cousin et al., 2005), are parametrized as two lognormal modes. Due to lack of knowledge on emitted particle sizes in each source category, the same distribution has been applied to all combustion sources. Emission mass distributions are mostly in a submicron (fine) mode (100% for BC and 60% for OCp), with a median diameter m of 0.23 μm and a dispersion coefficient σ of 1.89. A second (coarse) mode ($m = 2.5$ μm and $\sigma = 2.02$) contains the rest of OCp.

Due to coarse TM4 horizontal resolution, the same partition as in Cooke et al. (1999) was introduced, initially with 80/20% for hydrophobic / hydrophilic BC (resp. 50/50% for OCp), these ratios then evolving in time.

4. Simulations and comparative tests against worldwide measurements

4.1. General overview

BC and OC being the target aerosol components, two model versions have been used: the full ORISAM-TM4 including SOA formation and sectional microphysics and a reduced tracer version. In the following, OC calculated with the full ORISAM-TM4 refers to the sum of OCp (primary OC) and SOAc, with a distinction in SOAc between the anthropogenic (SOAAc) and biogenic (SOABc) fractions. 'c' indexes in 'SOAc', 'SOAAc' and 'SOABc' refer to quantities expressed in carbon mass. OC is also computed in the TM4 tracer version simulations, as primary OC multiplied by a constant empirical factor (1.25), which implies constant OCp/OC ratios. Both model versions were run from March 2002 to the end of August 2003, with 15-d spin up periods. Preliminary comparative tests were made between these model results and worldwide measurements at representative polar, temperate and tropical sites. Most generally, the tracer version appeared rather satisfactory for BC, but not for OC. For this latter, the full ORISAM-TM4 model was required to get more reliable comparisons between measurements and simulations.

4.2. Comparisons for BC

4.2.1. BC global distributions and budgets.

4.2.1.1. BC budgets. Modelled global yearly averaged BC burdens (Fig. 2) of 170 Gg are in the range of previous estimates amounting to 130 Gg (Liousse et al., 1996), 150–250 Gg (Cooke et al., 1999), 230 Gg (Jacobson et al., 2001b) and 120 Gg (Liu et al., 2005). Computed BC lifetimes, about 4.6 d, are also in

Table 3. Global yearly averaged BC (resp. OCp) emissions

Source type	Injection height	Seasonality	BC emissions (resp. OCp) (in TgC yr^{-1})
Fossil fuels (except Europe) (all types*)	<200 m	No (except for domestic fuel-use, monthly variations)	3.19 – 4.
Fossil fuels in European window (all types*)	<200 m	No (except for domestic fuel-use, monthly variations)	0.58 – 1.
Domestic biofuel combustion	< 200 m	Yes (monthly)	0.73 – 2.23
Agricultural fires	Temperate latitudes <4000 m, Other <200 m	Yes (monthly)	0.52 – 2.11
Forest and savanna fires in the Tropics	<1000 m	Yes (monthly)	2.49 – 18.33

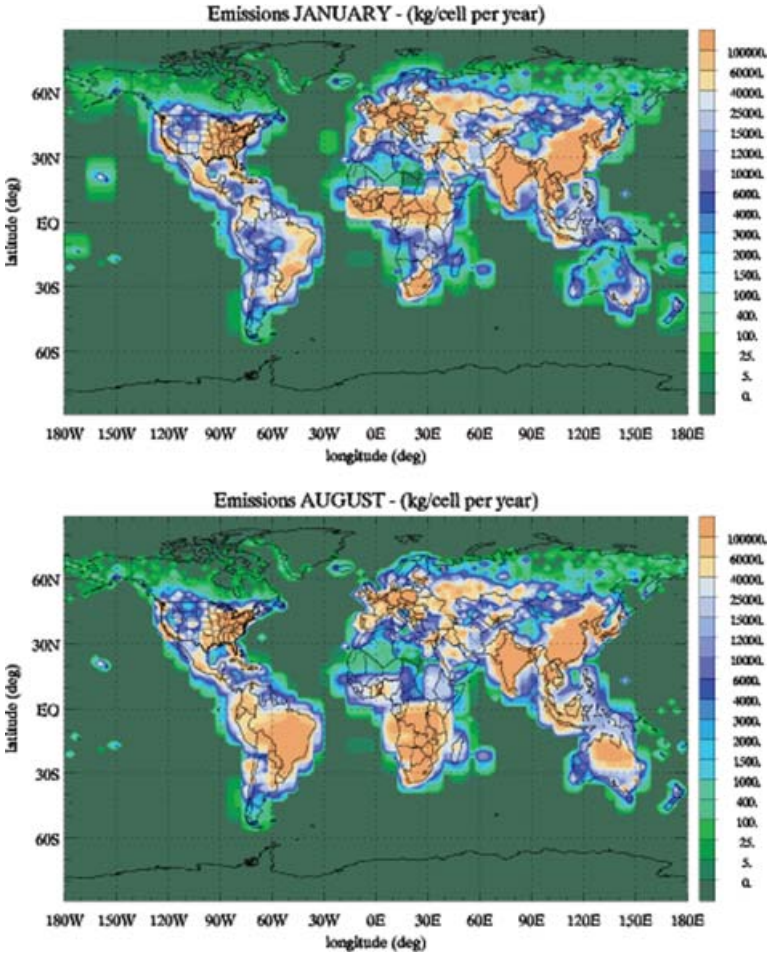

Fig. 1. BC emissions for January 2003 and August 2002 (resp. lower and upper frames).

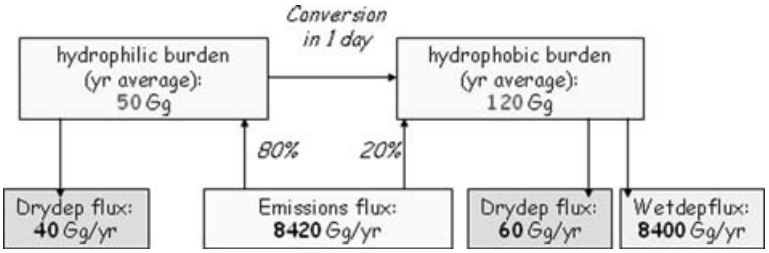

Fig. 2. Simulated BC global budgets.

the range of previous estimates. Differences with Liousse et al. (1996) appear in BC emissions and deposition. Here, emissions reach 8400 Gg yr^{-1}, compared to 12300 Gg yr^{-1} in Liousse et al. (1996), this difference being mainly due to tropical forest fires with emission factors (EF) lower by a factor 2 (cf. Section 3). Dry deposition fluxes are 100 Gg yr^{-1} against 3000 Gg yr^{-1} in Liousse et al. (1996), the deposition velocities being calculated here after Ganzeveld et al. (1998) as opposed to constant deposition velocities of 0.1 cm s^{-1}. Wet deposition is slightly lower, 8400 Gg yr^{-1} compared to 9300 Gg yr^{-1}.

4.2.1.2. BC global distributions. The global BC surface concentrations for August 2002 (upper frame) and January 2003 (lower frame) are displayed in Fig. 3. These concentrations reflect both the location of major BC emission sources of different origins (biomass burning, biofuels and fossil fuels) and also transboundary and transoceanic transport. Rather than proceeding to general comments on this Fig. 3, we concentrate on three particular major points in tropical areas. The first one concerns the interhemispheric seasonality of biomass burning over the African continent and its oceanic extent through emitted BC plumes. In January 2003 (dry season in the northern hemisphere), biomass burning in West and Central Africa generates a BC plume extending over the tropical Atlantic north of the Equator towards the south American continent, due to transport by the harmattan wind over the continent and the trade winds over the ocean. During this month, the high BC concentrations over South Africa (wet season

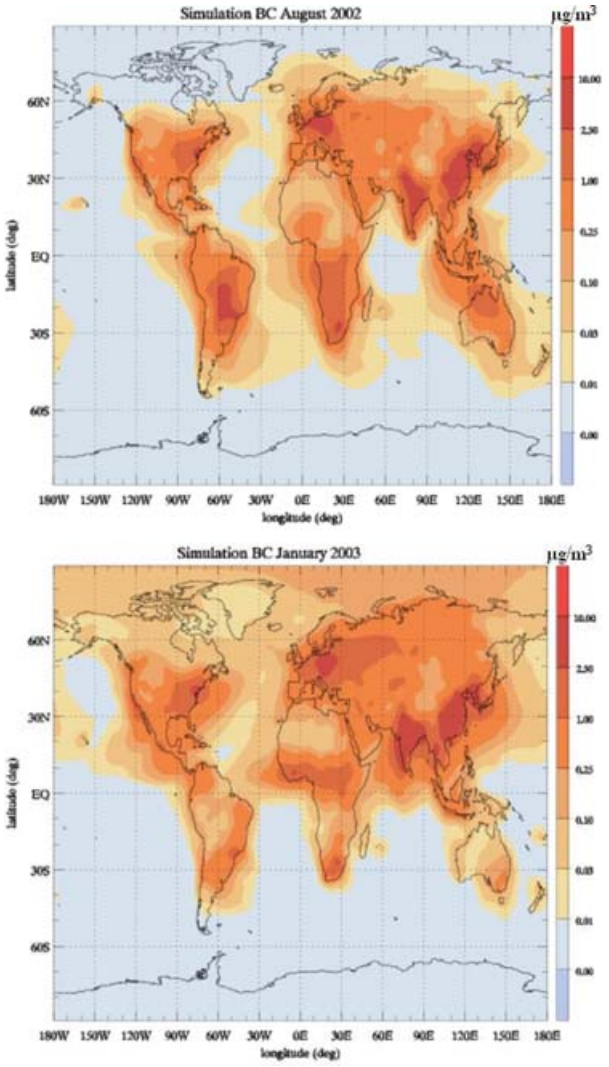

Fig. 3. Global simulated BC surface concentrations (in μg m^{-3}) in August 2002 and January 2003.

there) are possibly mainly due to fossil fuels and biofuels (urban and industrial) emissions, over Johannesburg and the industrial Vaal triangle. On the opposite, in August 2002 (dry season in the southern hemisphere), biomass burning is mostly developed in southern Africa, which generates BC plumes largely extending both over the south Atlantic and Indian Oceans, as can be seen in the upper frame in Fig. 3. Such situations are quite typical of summer/winter biomass burning emissions over Africa.

The second point to be underlined in Fig. 3 (upper frame) is about intense fires reported to affect Indonesia in August 2002: the resulting BC plume largely extends over southeast Asia, also reaching the north of Australia.

The third point is about the simulated extent of Indian pollution in January 2003 (winter monsoon) over the Indian Ocean and the Arabian Sea, studied during INDOEX (Lelieveld et al., 2001).

Further detailed discussions could be made for other geographical areas, such as Europe, China, the American continent, at this stage out of our present scope.

4.2.2. Simulated BC compared to observations at background and remote sites. BC simulations with the tracer version were tested against worldwide background and remote site observations. There were only few differences in BC when compared to Liousse et al. (1996) in these model/measurements comparisons, just slightly higher concentrations due to reduced deposition not entirely compensated by slightly lower emissions. However, updated inventories in the TM4 tracer version, together with improved precipitation rates (in the ERA40 reanalyses) have brought major improvements at some stations, as discussed below.

4.2.2.1. Amsterdam Island and the U.S. IMPROVE network. These comparisons are displayed at the remote Amsterdam Island station (Fig. 4) and at the background U.S. IMPROVE continental sites (Fig. 5). For BC at Amsterdam island, two vertical resolutions (9- and 19-levels) of the tracer version were tested against a set of monthly observations (minima and maxima values during the period 1991–1992–1993). The BC seasonal variations are well captured by the model, the highest resolution resulting in a doubling of the summer concentrations. In summer, the island is under the combined influence of the Mascarene subtropical anticyclone and biomass burning from southern Africa, pollutants from southern Africa being transported in thin layers better described in the highest TM4 vertical resolution. As for the North American IMPROVE network, there appears an overall satisfactory agreement between annually averaged model results and measurements. In particular, there is no overall underestimation as in Liousse et al. (1996), due to improved precipitation rates in the ERA-40 reanalyses. However, there are some overestimations at a few stations, e.g. at Mount Rainier, Point Reyes, Acadia and Pinnacles. At most of these stations, the

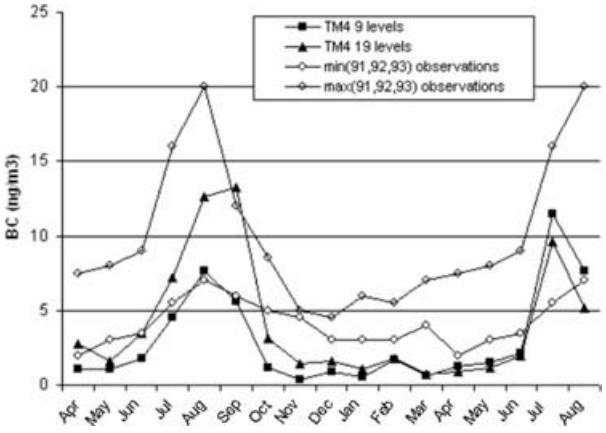

Fig. 4. Seasonal variations of modelled BC concentrations at Amsterdam island (April 2002 to August 2003) versus observed minima and maxima in 1991, 1992, 1993 – Vertical resolution in TM4 increased from 9 to 19 levels.

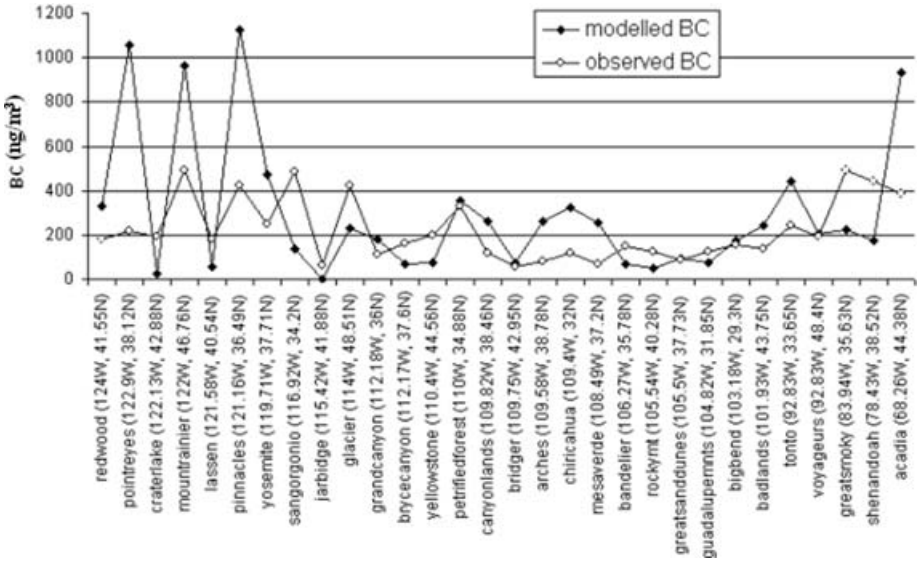

Fig. 5. Measured (yearly averaged over the period 1988-1991) vs. modelled BC surface yearly averaged concentrations (in ng m^{-3}) in the IMPROVE network (U.S. stations ordered from West to East).

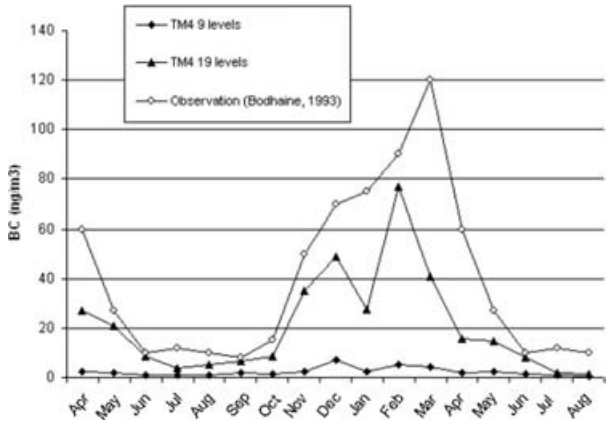

Fig. 6. Simulated BC concentrations at Barrow (April 2002–August 2003) compared to climatological data (Bodhaine, 1995) – Vertical resolution in TM4 increased from 9 to 19 levels.

overestimation is attributable to large urban centres within the same grid cell.

4.2.2.2. Arctic Haze. Arctic haze is a late winter/spring recurrent boundary layer phenomenon. This phenomenon clearly appears in Fig. 6 at Barrow (Alaska), particularly in March 2003 during the period of study. Also, this Fig. 6 illustrates the decisive improvement brought about in the boundary layer by the 19-level TM4 tracer version against the 9-level one. Arctic haze is due to the transport of European, Asian and North American pollution to boreal regions as can bee seen in Fig. 7(a), occasionally enhancing BC concentrations over Greenland up to 0.5 μg m^{-3}. A typical vertical BC profile (Summit site, 72°N, 38.5°W) over the Arctic for March 2003 is shown in Fig. 7(b).

4.2.2.3. BC wet deposition. Wet deposition is a major aerosol sink. Seasonal variations of precipitated BC at Enyele (Congo) and Lamto (Ivory Coast) are shown in Fig. 8. At both sites, the seasonal cycle is rather well captured by the model, with reduced BC amounts in April and October at Enyele and during the whole wet season in Western Africa at Lamto. At Enyele, the TM4 19-level version rather closely simulates the observed BC concentrations in rain, at the opposite of the nine-level one which clearly displays general overestimations. Fig. 9 displays global distributions of wet deposited BC (in μg l^{-1}) in January 2003 and August 2002. Marked collocation is observed between wet deposited BC and BC surface concentrations in Fig. 3. Also, the winter BC easterly flux from Africa to South America (cf. BC concentrations in Section 4.2.1) is manifest in wet deposited BC. In summer, BC heavily precipitates over the Gulf of Guinea due to widespread biomass burning sources in southern Africa.

4.2.3. BC concentrations near their sources: a zoom over Europe. BC surface concentrations are tightly driven by emission sources at their close vicinity, for instance in Europe. Several emission inventories are currently available, quite different in their characteristics and underlying assumptions, reflecting the large uncertainties still present in the current state of the art in this domain. First, the sensitivity of the TM4 tracer version was tested to such different BC emission inventories with comparisons to seasonal European observations. Secondly, the best performing and latest updated inventory has been retained for further comparisons with higher temporal resolution data from the EC/OC campaign (1-d samples collected per week).

4.2.3.1. Sensitivity tests using different European BC emission inventories. The four different European BC emission inventories in scenarios S1, S2, S3 and S4 described in Section 3 were tested in four different ORISAM-TM4 simulations using the

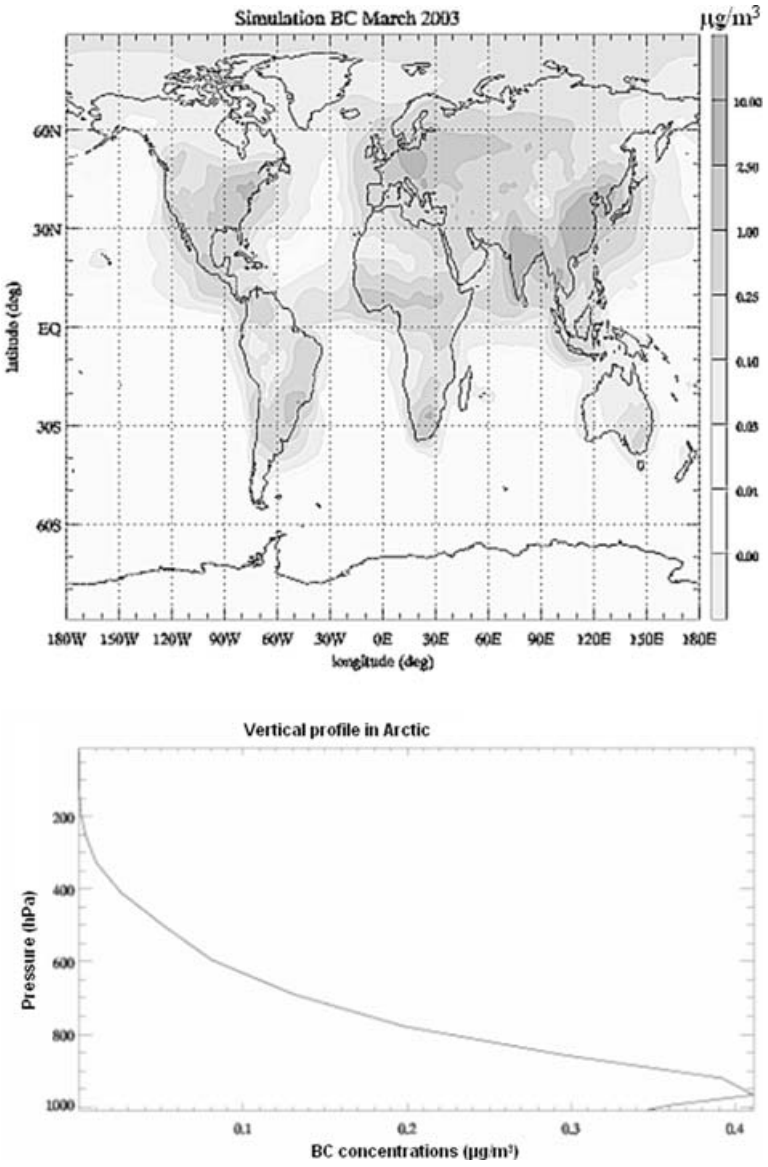

Fig. 7. (a) Global distributions of BC surface concentrations (in μg m^{-3}) in March 2003 and (b) Typical vertical BC profile in the Arctic region (Summit –72°N, 38.5°W) in March 2003.

tracer version. S1, S2, S3 and S4 simulations were performed over the period March 2002–August 2003. Simulated BC concentrations were then compared to a review of experimental BC data quoted in Solmon et al. (2006). Scatter plot diagrams between simulated and observed BC were drawn, rather similar for the summer and winter periods: these diagrams are thus displayed in Fig. 10 only for the summer 2002. Though an important factor of dispersion is inherently due to coarse ($3^\circ \times 2^\circ$) model resolution resulting in low correlation coefficients, the relative quality of model results is given by the proximity of regression line slope to 1. In Fig. 10, S2 scenario (regression line slope near 0.8) clearly appears as the best performing of all four scenarios. For S3 and S4 scenarios (regression line slope near 0.5), with large uncontrolled emission proportions in the inventories, the model overestimates the observed BC concentrations by a factor of two, slightly higher but still in general agreement with the results of processing of Cooke et al.'s (1999) emissions using the RegCM model over Europe (Solmon et al., 2005). As for S1 (regression line slope near 1.6), with lower uncontrolled emission proportions, severe underestimations reach as much as 70%, confirming previous results of S1 emission processing by LOTOS model over Europe (Schaap et al., 2004). With higher uncontrolled emissions than S1 but also integrating more detailed controlled emissions than S3 and S4, simulated and observed BC concentrations in S2 scenario much more agree, with only 20% underestimation. These results clearly show better agreement when considering in BC inventories a high fraction of uncontrolled emissions, even though in Europe

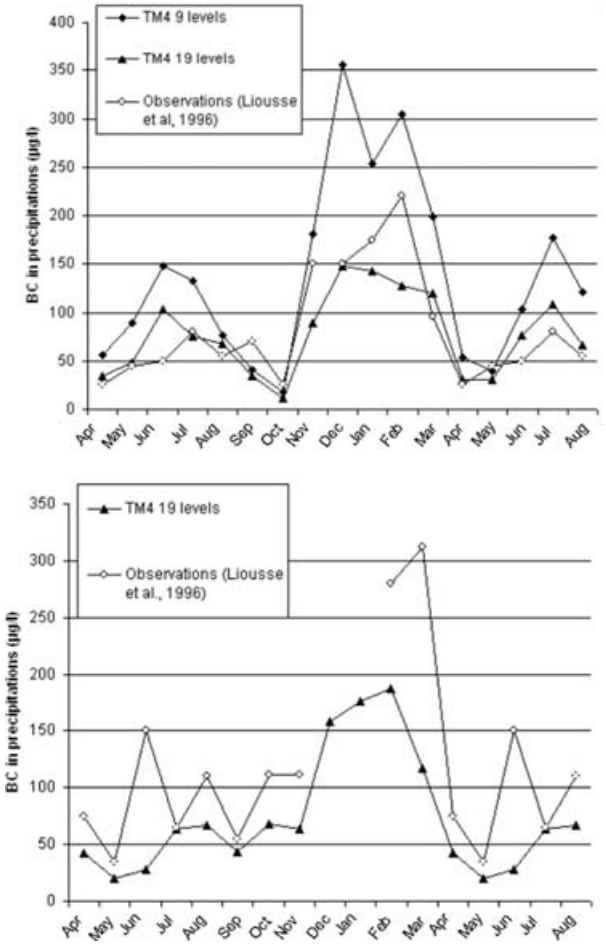

Fig. 8. (a) Seasonal variations of BC concentrations in precipitation (in μg l^{-1}) at: (a) Enyele (Congo), (b) Lamto (Ivory Coast) - Vertical resolution in TM4 increased from 9 to 19 levels.

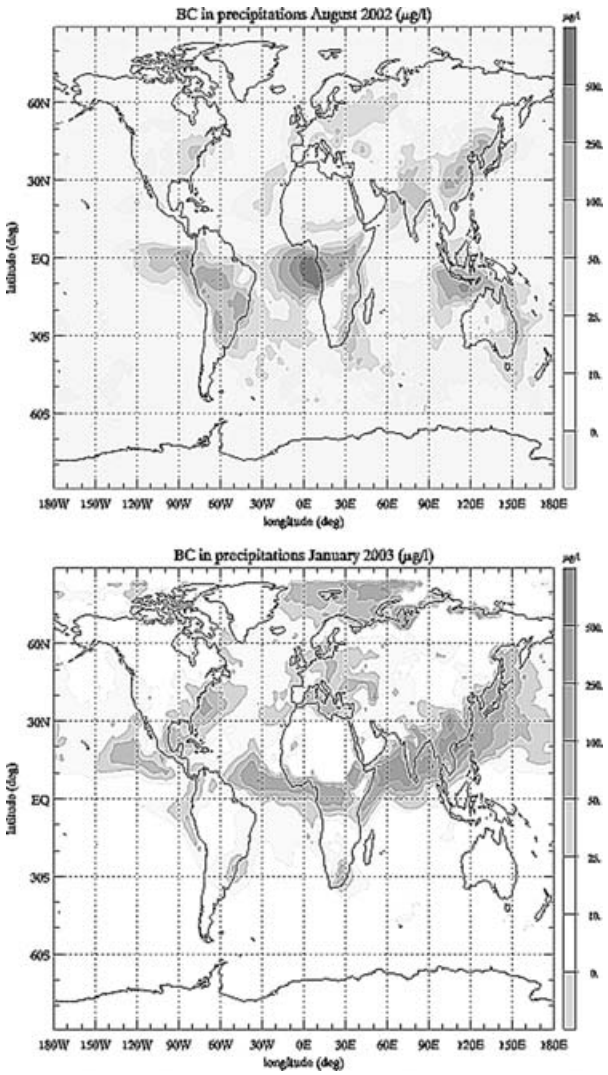

Fig. 9. Global simulated distribution of wet deposited BC (in μg l^{-1}) in August 2002 and January 2003 (resp. upper and lower frames).

anti-pollution norms are (at least partially) applied to particle emissions.

4.2.3.2. One-day samples weekly collected during the EC-OC campaign. Finer time resolution data for comparisons between modelled and measured BC concentrations were collected during the EC/OC Campaign (Kahnert, 2002) of the Co-operative Programme for Monitoring and Evaluation of the Long-range Transmission of Air pollutants in Europe (EMEP program). One-day samples per week have been collected during the period from July 2002 to July 2003, simultaneously at nine cities of the EMEP network. Comparisons with modelled BC concentrations at five cities are shown in Fig. 11. The model correctly reproduces average values (not the peaks) at Aspvreten, Braganca and Ispra and their evolution in time, though stronger seasonality is found at Ispra in the observations than in modelled concentrations. At Kollumerwaard and Virolahti, the model overestimates BC concentrations, due both to coarse horizontal model resolution (especially in the Netherlands densely packed urban network) and slightly too high emissions in Northern Europe (Scandinavia, Germany, Netherlands) in the Guillaume and Liousse's (2006) BC low scenario.

4.3. Simulated vs. observed OC using the full ORISAM-TM4 model

4.3.1. Overview over OC.

4.3.1.1. OC burdens. Few global models deal with primary and SOAs, particularly with a discrimination between anthropogenic and biogenic SOA. Available global OC budgets and lifetimes in literature and the present one are displayed in Table 4. For the secondary fraction, a comparison is made with SOA implemented within TM3 (Tsigaridis and Kanakidou, 2003). Among the different cases simulated by these latter authors, their case S2 has the closest assumptions to those in ORISAM-TM4. This

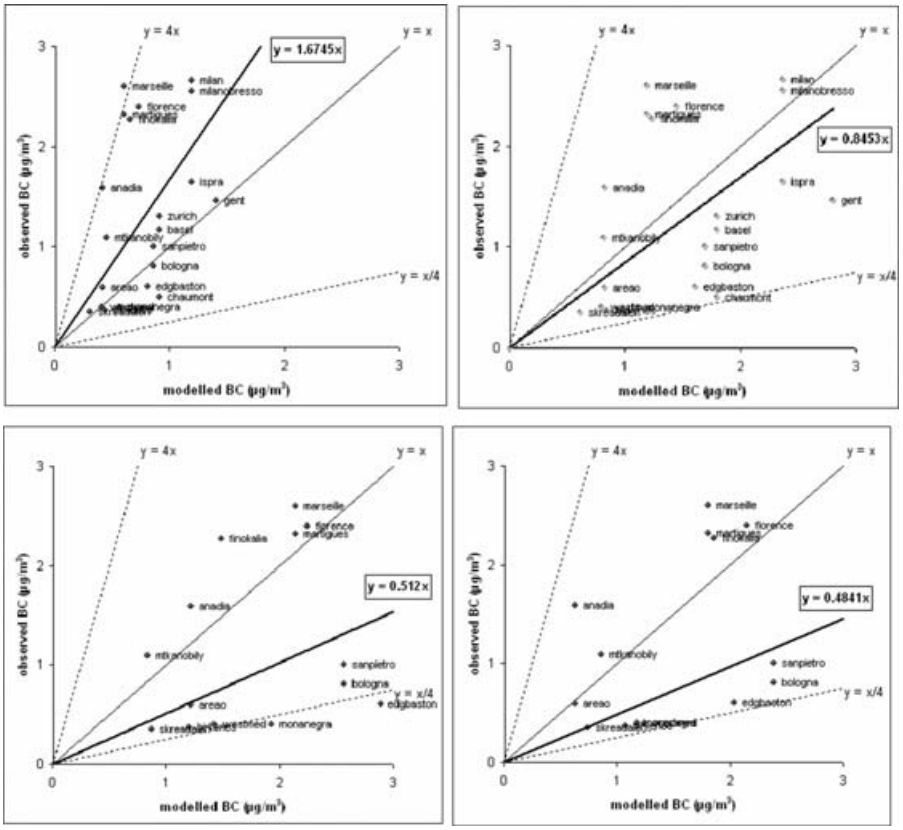

Fig. 10. Scatter plot diagrams of modelled vs. observed BC concentrations (in μg m^{-3}) for summer 2002 in the (a) S1, (b) S2, (c) S3 and (d) S4 simulations.

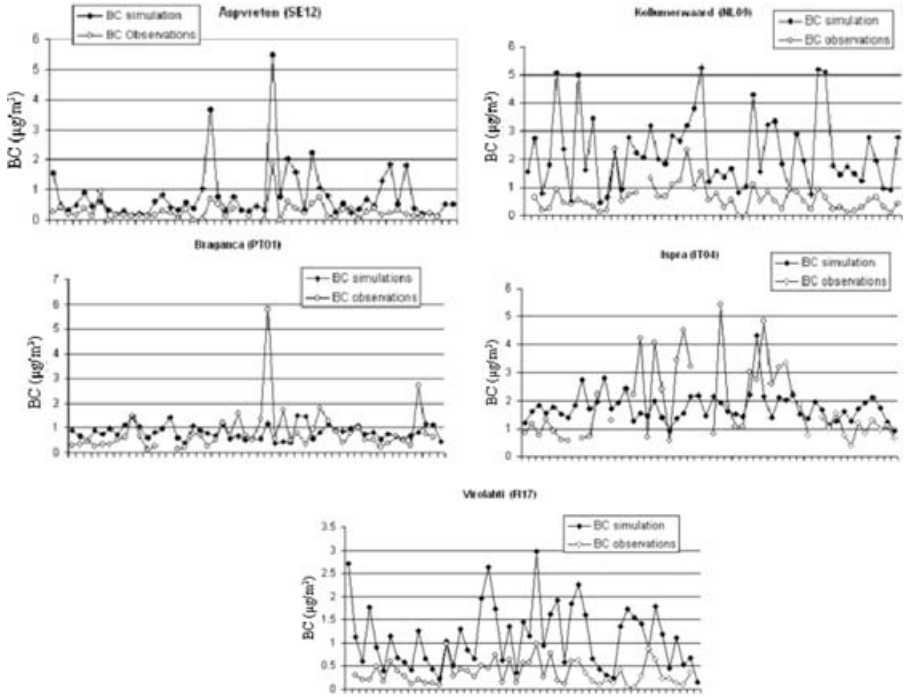

Fig. 11. BC concentrations from 1-d samples collected weekly at selected EMEP stations during the EC/OC campaign (July 2002–July 2003).

Table 4. Global OC yearly-averaged burdens

OC	Global burden in Gg yr average (and lifetime in days)	Global burden in Gg yr average (and lifetime in days)	Source
Total OC-tracer	588 (4.5 d)	736–738 (3.2 d)	Liousse et al. (1996), Jacobson (2001), Liu et al. (2005)
Total ORISAM-TM4 OC	1020 (3.9 d)		
Primary OC (OCp)	470 (4.5 d)		
Anthropogenic SOAc	50 (3 d)	24.6[a]	Tsigaridis and Kanakidou (2003)
Biogenic SOAc	500 (2.9 d)	370[a]	Tsigaridis and Kanakidou (2003)

[a]Burdens from case S2 in Tsigaridis and Kanakidou (2003).

comparison lets appear higher SOABc and SOAAc in TM4, possibly due to the main difference between these two models, namely the additional feature in ORISAM-TM4 of size-distributed SOA. In TM3, evidence was found of a dominant biogenic origin for SOAc, confirmed here with 500 Gg for biogenic against 50 Gg for anthropogenic SOAc. Likely, reevaluation of these estimates, with more detailed SOA anthropogenic precursors (e.g. long-chain alkanes) would still be necessary, since underestimations have been found for instance between modelled and measured results in the urban/industrial area near Marseilles (France) (Cousin et al., 2005). More generally, such effects on SOA formation could impact continental budgets, due to the growth of large urban/industrial sites. As for total OC, comparisons are made here with a set of three references: Liousse et al. (1996), Jacobson (2001b) and Liu et al. (2005). These authors use an OM-tracer model where OM is organic matter, with OM burdens being related to OC ones by a 1.3 multiplication factor (Liousse et al., 1996) accounting for H/C ratios. OC burdens from these authors have similar values (736–738 Gg), since they use only slightly different transport schemes processing the same OM emission inventory, after Liousse et al. (1996) for biomass burning and after Cooke et al. (1999) for fossil fuels sources. They show higher values than OC burdens here with OC-tracer (588 Gg) due to significantly lower emissions in the inventory used here (cf. Section 3). OC burdens in ORISAM-TM4 (1020 Gg) are higher than OC-tracer burdens, due to a higher part of SOA in total OC, OC-tracer being invariably given by OC = 1.25*OCp while in ORISAM-TM4, OC is allowed to vary.

4.3.1.2. Global distributions of OCp and SOAc. Global distributions of OCp, of the anthropogenic (SOAAc) and biogenic (SOABc) fractions of secondary OC for August 2002 are displayed in Fig. 12. High OCp values are observed over Central Europe and Asia (China and India), as well as over the tropics (intense forest and savanna fires in Amazonia, in southern Africa and in Indonesia). Interestingly, in West Africa, August maxima SOABc values are not strictly collocated with the vegetation cover but somewhat advected by southern fluxes towards the ITCZ (then located near 20°N). High SOAc values are found in the latitude range 0°–5°N, with model predicted SOAAc about 10 times lower than SOABc.

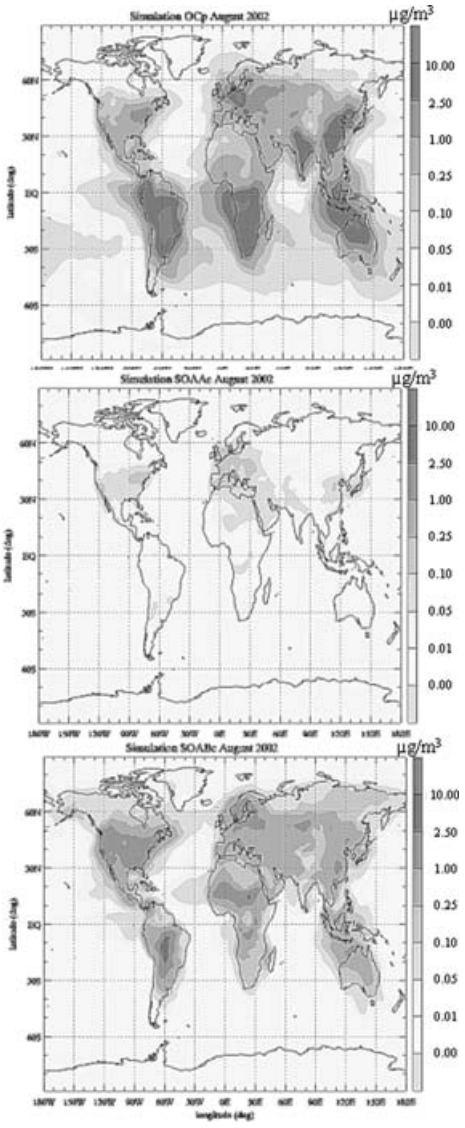

Fig. 12. Global distributions in August 2002 of: (a) OCp (upper frame); (b) SOAAc (left lower frame) and (c) SOABc (right lower frame).

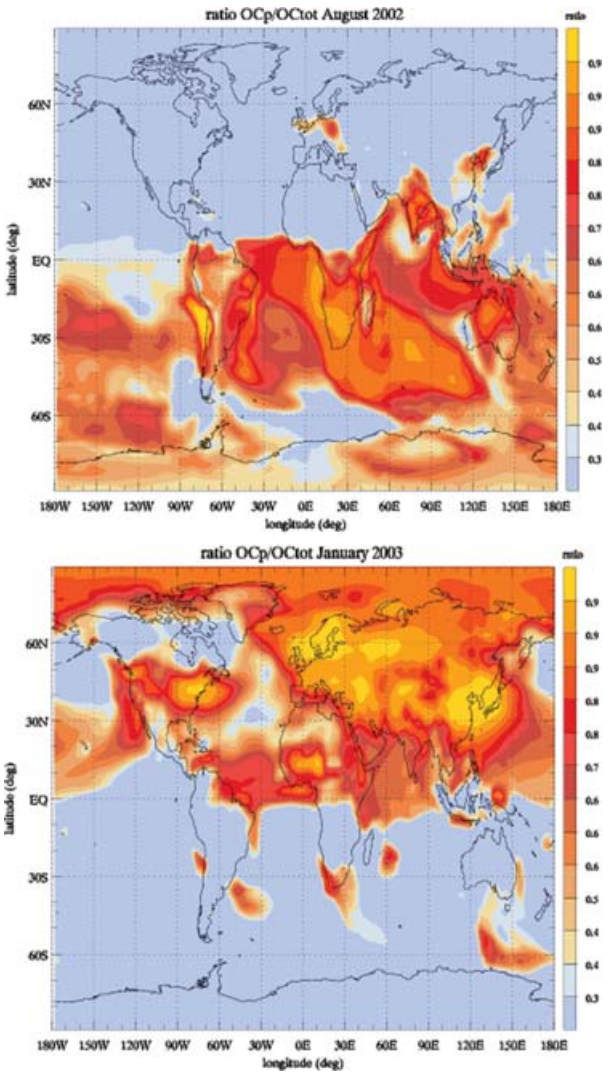

Fig. 13. OCp/OCtot ratios in August 2002 and January 2003.

4.3.1.3. OC modelling improvements due to ORISAM. One new major improvement due to ORISAM implementation in TM4 is in the seasonal variations of the ratios OCp/OC shown in Fig. 13, for August 2002 and January 2003. With OCp/OC values in the range 0.35–1, global averaged OCp/OC ratios are about 0.45 in August 2002 and 0.55 in January 2003, in close agreement with previously reported SOA/OC ratios (Fuzzi et al., 2005). Now turning to hemispheric differences, OCp predominates in summer in the southern hemisphere (less active photochemistry) whereas in winter, OCp is predominant in the northern hemisphere. More precisely, in summer high OCp/OC ratios (about 0.8) are found in August 2002 in the southern hemisphere (mainly due to intense OCp emissions by savannas and forests fires), in Asia (China and India) and in Central Europe. On the opposite, over areas strongly emitting biogenic SOA (North America, Africa south of the ITCZ) and over the oceans (Atlantic, Mediterranean sea and West Pacific), summer OCp/OC ratios are most often below 0.4. In winter, VOC photochemistry being less active and OCp enhanced (domestic heating), OCp/OC ratios are mostly above 0.8 in the northern hemisphere, especially over Europe. In the southern hemisphere, biogenic VOC emissions strongly enhance SOABc, thus decreasing OCp/OC ratios. These seasonal interhemispheric inversions are particularly clear over Africa in Fig. 13. These results are hampered by large uncertainties in OCp emissions and also on SOA formation, due to still poor knowledge on the anthropogenic and biogenic species involved in successive VOC oxidation steps leading to condensable products and their aerosol yield values, in particular for long-chain alkanes, not yet considered here. Moreover, an important issue concerns anthropogenic VOC emissions from biomass burning used here, with emission factors (Andreae and Merlet, 2001) issued from aircraft measurements ('aged' particles) underestimated since not near fresh ground sources (some SOA formation already happened). On-going research is still in progress.

4.3.2. OC at background and remote sites. In aerosol models with no SOA formation (e.g. the TM4-tracer version), OC as a tracer is usually estimated as 1.25*OCp. Comparisons between annual OC observations and OC both simulated as a tracer with TM4-tracer and simulated with the full aerosol ORISAM-TM4 are shown in Fig. 14 at the stations of the IMPROVE network. OC as a tracer clearly underestimates the observations by an average factor of 4 at all stations, whereas OC from ORISAM-TM4 more closely agrees with the observations, with 5% differences only. This latter model predicts large SOA fractions (86%) at most stations, the higher fractions being in the Northern and Central Rockies. Some few overestimations appear, particularly at coastal sites and over the Colorado plateau, while underestimates are mostly found at eastern U.S. sites. This model predicts largely predominant fractions of biogenic SOA (80% on average at all sites), though with the restriction of some anthropogenic VOC precursors missing.

4.3.3. OC near their sources (European zoom).

43.3.1. OC seasonal averages. OCp emissions and SOA formation are two basic ingredients in total OC, observed and modelled, both subject to several limitations. First, OC observations cannot discriminate between primary and secondary OC, an advantage for OC modelling which allows such a distinction. A second limitation is in high uncertainties in OCp emissions. A third one is in SOA modelling, still hampered by lack of knowledge on anthropogenic and biogenic precursors and their reaction pathways. However, in spite of these limitations, comparisons were made over Europe, an intense OC source region, between modelled and observed concentrations (Fig. 15), these latter based on a review of experimental OC data by Solmon et al. (2005). The same stations have been selected in winter and in summer covering the whole European continent, ordered in Fig. 15 from west to east. Two stations (Krvavec near Ljubljana and K-puszta in Hungary) display singular overestimated modelled values, not

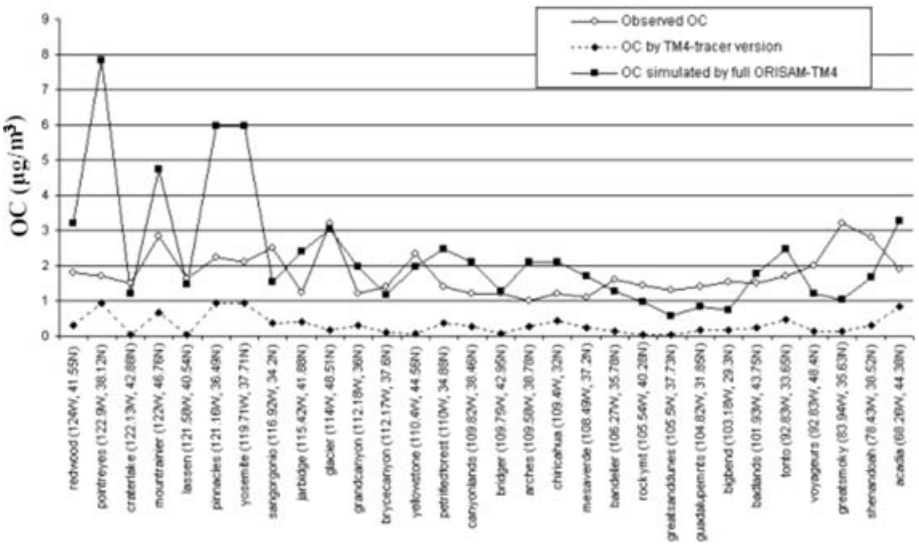

Fig. 14. Yearly averaged OC observations in the IMPROVE network compared to modelled OC (both by TM4-tracer and the full ORISAM-TM4).

further considered. Clearly, a difference appears at all other stations between summer and winter simulations, due to enhanced SOA formation in summer by photochemistry: this explains the largest difference then between OC-tracer below OC issued from ORISAM-TM4. Also, though this difference is much smaller in winter, one then observes slightly higher values in OC-tracer (invariably 1.25*OCp) against OC from the full ORISAM-TM4. In these comparisons between simulations and measurements, a discrimination has to be made between winter (Fig. 15a) and summer (Fig. 15b). In winter, as already quoted, there is only a slight difference between OC-tracer and the full-ORISAM OC and rather close proximity to observations. For instance, modelled OC averaged all over European sites amounts up to 1.73 μg m^{-3} for ORISAM-TM4, 1.85 μg m^{-3} for OC-tracer, against observed 1.31 μg m^{-3}. Now turning to summer 2003 (Fig. 15b), the behaviour of both simulations vs. observations is more complex and contrasted over Europe than over mostly background stations of the IMPROVE network (Fig. 14), in particular due, as already the case for BC, to closer proximity between sources and measurement sites. Three different behaviours can thus be depicted. First, the stations where ORISAM-TM4 satisfactorily simulates observed OC at the difference of OC-tracer: this is the case at Anadia, Marseilles, Paris, Milan, Florence and Finokalia. Secondly, stations where OC-tracer more favourably compares to observations than the full ORISAM, such as Areao, Basel, Ispra, Bologne possibly mainly due to too enhanced biogenic SOA formation in ORISAM-TM4. Thirdly, stations such as Mace Head, Chaumont, Birkenes, where even the OC-tracer is unsatisfactory, pointing out to overestimated local emissions. This latter situation was already pointed out in the comparisons between BC simulations and measurements. In such a complex domain as Europe with close proximity between sources and stations, these different behaviours highlight the advantage of using the full ORISAM model (with SOA formation), but also the limitations due to the needs for still improved detailed emission inventories together with improved knowledge on VOC precursors and SOA formation.

4.3.3.2. Weekly collected 1-d samples (EC-OC campaign). Finally, Fig. 16 shows OC modelled (using both TM4-tracer and the full ORISAM-TM4) and measurement comparisons during the EC/OC Campaign, restricted to August 2002 and January 2003 at four representative EMEP stations (Virolahti (FI), Ispra (IT), Kollumerwaard (NL) and Braganca (PT)). In this Fig. 16, as previously the case for BC (Fig. 11), week-to-week measurements at these sites are generally rather favourably captured, both by the OC-tracer and by the full-ORISAM-TM4. In summer (Fig. 16b), the advantage of this latter against OC-tracer appears in the correctly modelled relative contributions of SOA to OC, except at Kollumerwaard (NL) where OC overestimation is likely related to OCp emissions. In winter (Fig. 16a), quite large measured OC values (even higher than in summer) appear at Ispra and Braganca. This experimental 'cold OC' still remains unexplained, before comparisons with modelled values.

4.4. Size distributions of carbonaceous aerosols

Simulated aerosol size distributions have been reported for inorganic species, but only few studies deal with carbonaceous aerosols: here, this is one of the few attempts at global sectional modelling of carbonaceous aerosols, involving BC, OCp and SOA formation. Lack of data most generally hampers systematic model to measurements comparisons, though some experimental data appear to be available. As a preliminary modelling result, Fig. 17 displays yearly averaged size differentiated aerosol

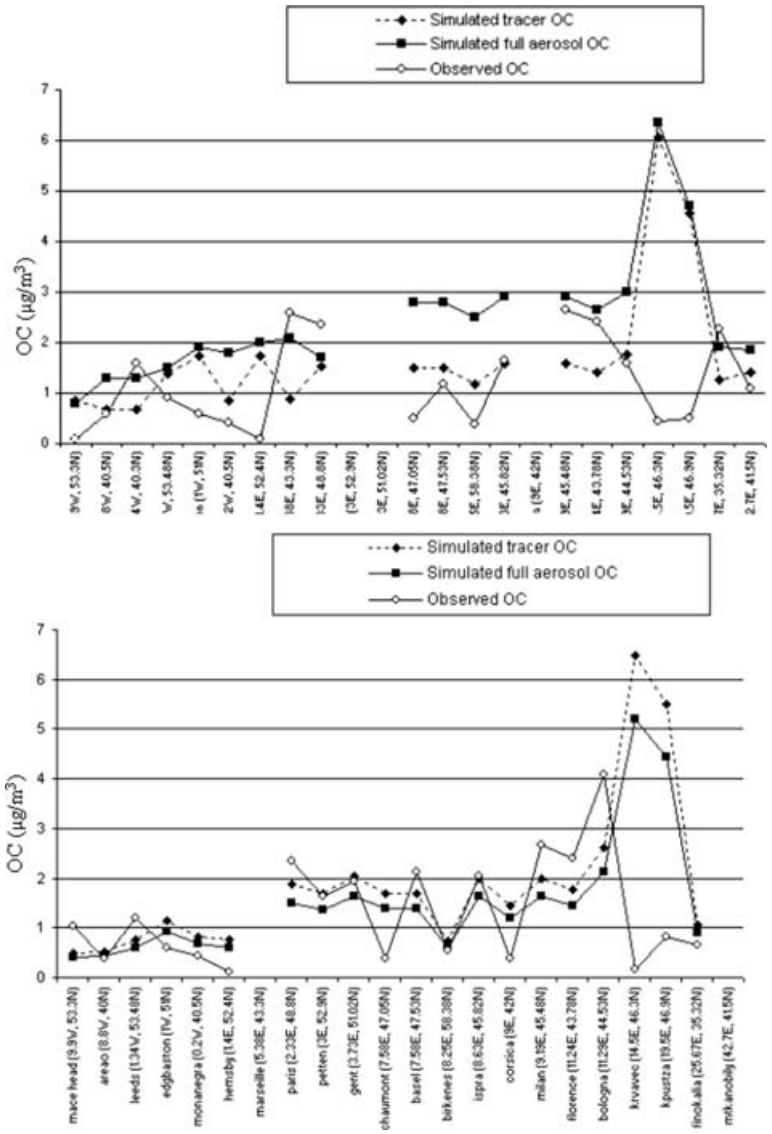

Fig. 15. Seasonal averages of OC concentrations (in μg m^{-3}), measured and modelled (both by TM4-tracer and by full ORISAM-TM4): (a) in winter and (b) in summer.

burdens (in GgC) at the global scale (Fig. 17a) and over Europe (Fig 17b). The three following components are discriminated: BC, OCp and SOAc. ORISAM-TM4 predicts primary (BC and OCp) particle ratios, respectively, about 39% (global scale) and 48% (Europe) against total carbonaceous aerosol mass, mostly due to less biogenic SOA formation in Europe. Now, when scrutinizing at detailed chemical speciation between bins, two salient features appear. First, both at global scale and over Europe, SOA formation occurs at small sizes (e.g. below 0.9 μm) while OCp particles are spreaded more uniformely in the range 0.2–5 μm. Secondly, OCp/BC ratios are higher at the global scale than in Europe due to different predominant emission combustion types, fossil fuels in Europe and vegetation fires globally (Guillaume and Liousse, 2006; Junker and Liousse, 2006). Further simulations and measurements are still required.

5. Conclusions and Prospects

A new global aerosol model is presented, coupling the sectional aerosol model ORISAM to the CTM TM4. Due adaptations for this implementation have been detailed, before focusing upon aerosol components, BC, OCp and SOA formation. In close connection with this focus, new updated BC and OCp fossil fuel emission inventories for Europe and at the global scale have been tested in the model. In particular, processing European emission inventory with more realistic fractional controlled/uncontrolled emission scenarios in the ORISAM-TM4 tracer version has resulted in better agreement between model results and observations. Due to different predominant carbonaceous aerosol emission sources, BC/OCp ratios modelled by ORISAM-TM4 (Fig. 17) are higher in Europe than at the global

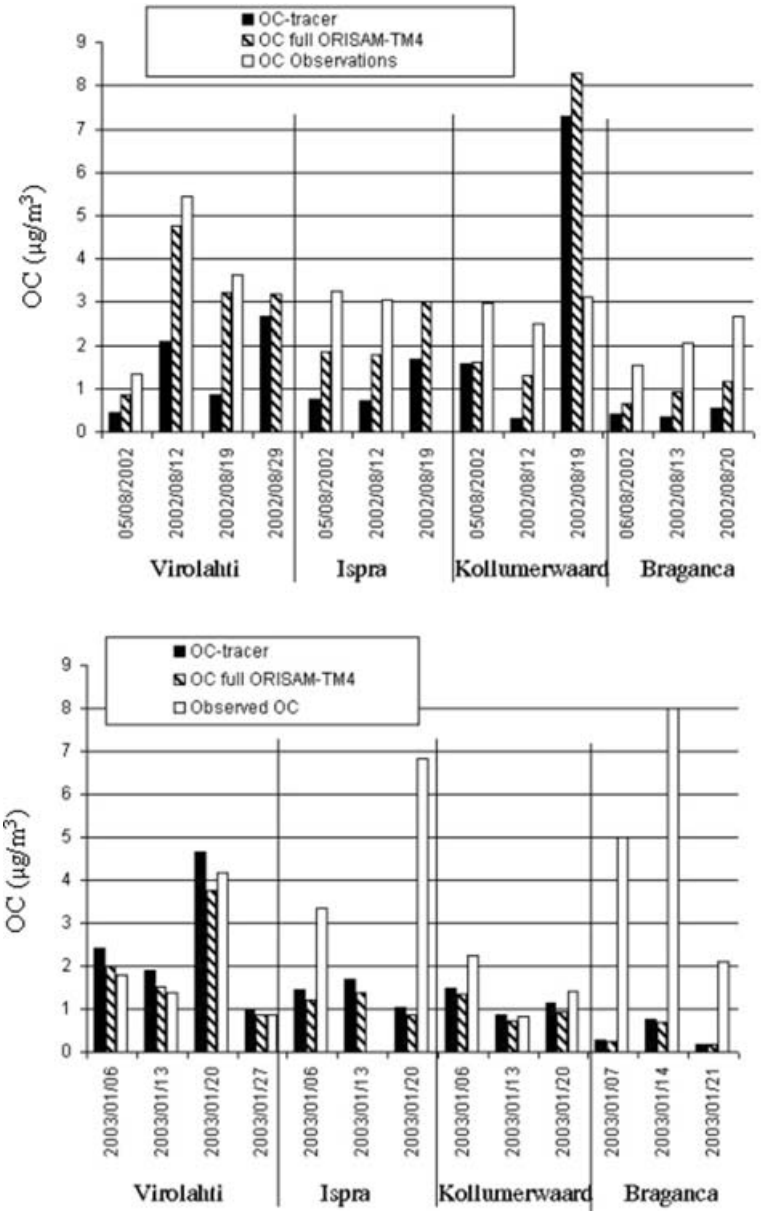

Fig. 16. OC concentrations (in μg m^{-3}) from 1-d samples weekly collected during EC/OC campaign at four different EMEP stations: (Virolahti (FI17), Ispra (IT04), Kollumerwaard (NL09) and Braganca (PT01)): (a) in winter and (b) in summer.

scale. Whenever SOA formation is active (e.g. in summer), the full ORISAM-TM4 model significantly improves the TM4-tracer results. Such formation displays large variations, between 5 and 65% of the total aerosol mass, strongly dependent on location and season: as shown in Fig. 13, ORISAM-TM4 allows to get rid of the constraint of imposed OCp/OC ratios sometimes used in global aerosol models, thus quantifying the variable relative importance of secondary organics. Also, comparison in Fig. 17 between global and European size-segregated organic species further highlights the regional differences on carbonaceous aerosols. At this stage, several prospects can be considered. To quote just a few, VOC precursors, their transformations and aerosol yields are still a key domain with several particular issues, such as the role of isoprene and detailed classes of anthropogenic VOC precursors (e.g. long-chain alkanes/alkenes) in SOA formation. Also, coupling between inorganics and organics within internally mixed aerosols have to be developed for improving hygroscopic (e.g. ageing effect) and radiative aerosol properties, together, most generally, with aerosol-cloud interactions. Of course, regular emission inventory updating remains a basic recurrent need, together with extensive chemically speciated size-differentiated aerosol measurements.

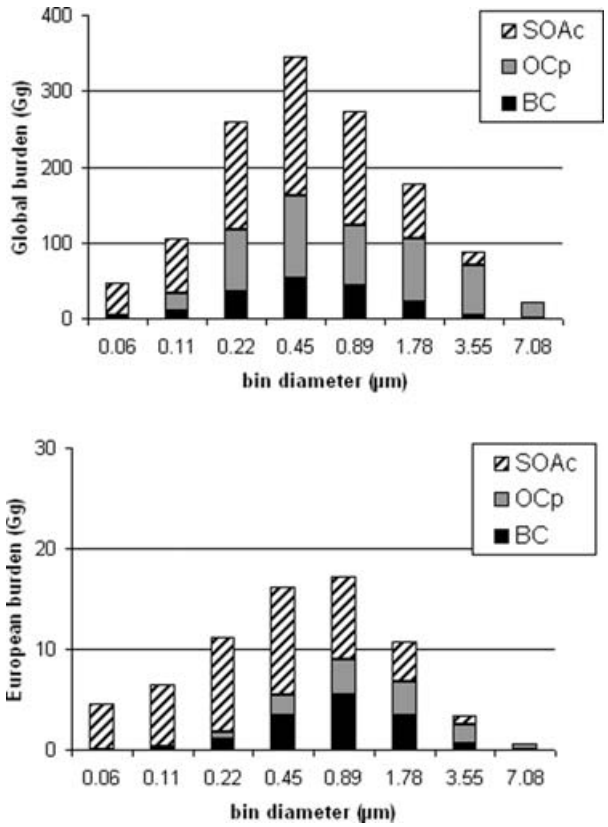

Fig. 17. Yearly averaged burdens (in Gg) of size-differentiated carbonaceous aerosols (a) at global scale and (b) over Europe.

References

Adams, P. J. and Seinfeld, J. H. 2002. Predicting global aerosol size distributions in general circulation models. *J. Geophys. Res.* **107**(D19), 4370, doi:10.1029/2001JD001010.

Adams, P. J., Seinfeld, J. H. and Koch, D. M. 1999. Global concentrations of tropospheric sulphate, nitrate and ammonium aerosol simulated in a GCM. *J. Geophys. Res.*. **104**, 13791–13823.

Andreae, M. O. and Merlet, P. 2001. Emission of trace gases and aerosols from biomass burning. *Global Biogeochemical Cycles*. **15**, 955–966.

Bessagnet, B., Hodzic, A., Vautard, R., Beekmann, M., Cheinet, S. and co-authors. 2004. Aerosol modelling with CHIMERE- preliminary evaluation at the continental scale. *Atmos. Environ*. **38**, 2803–2817.

Binkowski, F. S. and Shankar, U. 1995. The regional particulate matter model – 1. Model description and preliminary results. *J. Geophys. Res.* **100**, 26191–26209.

Bond, T. C. and Sun, H. 2005. Can reducing black carbon emissions counteract global warming?. *Environ. Sci. Technol.*. **39**, 5921–5926.

Bond, T. C., Streets, D. G., Yarber, K. F., Nelson, S. M., Woo, J.-H. and co-authors. 2004. A technology-based global inventory of black and organic carbon emissions from combustion. *J. Geophys. Res.*, **109**, D14203, doi:10.1029/2003JD003697.

Cachier, H. 1998. Carbonaceous combustion aerosols. In: *Atmospheric particles* (eds R. M. Harrison and R. Van Grieken). John Wiley and Sons Ltd, New York. 295–348.

Chin, M., Jacob, D. J., Gardner, G. M., Foreman-Fowler, M. S., Spiro, P. A. and co-authors, 1996. A global three-dimensional model of tropospheric sulphate. *J. Geophys. Res.* **101**, 18667–18690.

Cooke, W. F., Liousse, C., Cachier, H. and Feichter, J. 1999. Construction of a $1^\circ \times 1^\circ$ fossil-fuel emission dataset for carbonaceous aerosol and implementation en the ECHAM4 model. *J. Geophys. Res*. **104**, 22137–22162.

Cooke, W. F., Ramaswamy, V. and Kasibhatla, P. 2002. A general circulation model study of the global carbonaceous aerosol distribution. *J. Geophys. Res.* **107**(D16), doi:10.1029/2001JD001274.

Cousin, F., Liousse, C., Cachier, H., Bessagnet, B., Guillaume, B. and co-authors. 2005. Aerosol modelling and validation during Escompte 2001. *Atmos. Environ*. **39**(8), 1539–1550.

Dana, M. T. and Hales, J. M. 1976. Statistical aspects of the washout of polydispers aerosols. *Atmos. Environ*. **10**, 45–50.

Dentener, F. J. and Crutzen, P. J. 1994. A global 3D model of the ammonia cycle. *J. Atmos. Chem*. **19**, 331–369.

Dusek, U., Frank, G. P., Hildebrandt, L., Curtius, J., Schneider, J. and co-authors. 2006. Size matters more than chemistry for cloud-nucleating ability of aerosol properties. *Science*. **312**, 1375–1378.

Ervens, B., Feingold, G., Frost, G. J., Kreidenweis, S. M. 2004. A modelling study of aqueous production of dicarboxylic acids: 1/ Chemical pathways and speciated organic mass production. *J. Geophys. Res*. **109**, D15205.

Fuzzi, S., Andreae, M. O., Huebert, B. J., Kulmala, M., Bond, T. C. and co-authors. 2005. Critical assessment of the current state of scientific knowledge, terminology, and research needs concerning the role of organic aerosols in the atmosphere, climate and global change. *Atmos. Chem. Phys. Discuss.* **5**, 11729–11780.

Ganzeveld, L., Lelieveld, J. and Roelofs, G.-J. 1998. A dry deposition parameterization for sulfur oxides in a chemistry and general circulation model. *J. Geophys. Res*. **103**, 5679–5694.

Gelbard, F., Tambour, Y. and Seinfeld, J. H. 1980. Sectional representations for simulating aerosol dynamics. *J. Colloid Interface Sci*. **76**, 541–556.

Guelle, W., Balkanski, Y., Dibb, J., Schulz, M. and Dulac, F. 1998. Wet deposition in a global size-dependent aerosol transport model. 2, Influence of the scavenging scheme on 210Pb vertical profiles, surface concentrations, and deposition. *J. Geophys. Res.*. **103**, 38875–28891.

Guillaume, B. and Liousse, C. 2006. Development of carbonaceous aerosol emission inventories from fossil fuel over Europe at continental scale with focus on traffic at national and regional scales. *ADEME (French Ministery of Environment and Sustainable Development) Report. Project 0262050*.

Haywood, J. M., Roberts, D. L. Slingo, A., Edwards, J. M. and Shine, K. P. 1997. General circulation model calculations of the direct radiative forcing by anthropogenic sulphate and fossil-fuel soot aerosol. *J. Clim*. **10**, 1562–1577.

Heald, C. L., Jacob, D. J., Park, R. J., Russell, L. M., Huebert, B. J. and co-authors. 2005. A large organic aerosol source in the free troposphere missing from current models. *Geophys. Res. Lett.* **32**, L18809, doi:10.1029/2005GL023831.

Heintzenberg, J., Charlson, R. J., Clarke, A. D., Liousse, C., Ramaswamy, V. and co-authors. 1997. Measurements and modelling of aerosol single-scattering albedo: Progress, problems and prospects. *Beitr. Phys. Atmos.* **70**, 249–263.

Hertel, O., Berkowicz, R., Christensen, J. and Hov, O. 1993. Test of two numerical schemes for use in atmospheric transport-chemistry models. *Atmos. Environ.* **27A**, 2591–2611.

Heymsfield, A. J. and Donner, L. J. 1990. A scheme for parameterizing ice-cloud water content in general circulation models. *J. Atmos. Sci*. **47**, 1865–1877.

Houweling, S., Dentener, F. and Lelieveld, J. 1998. The impact of non-methane hydrocarbon compounds on tropospheric photochemistry. *J. Geophys. Res*. **103**, 10673–10696.

Jacob, D. J. 2000. Heterogeneous chemistry and tropospheric ozone. *Atmos. Environ*. **34**, 2131–215.

Jacobson, M. Z. 1999. *Fundamentals of Aerosol Modelling*. Cambridge University Press, Cambridge. 526–537.

Jacobson, M. Z. 2001a. GATOR-GCMM: A global- through urban-scale air pollution ad weather forecast model, 1. Model design and treatment of subgrid soil, vegetation, roads, rooftops, water, sea ice and snow. *J. Geophys. Res.*. **106**, 5385–5402.

Jacobson, M. Z. 2001b. Global direct radiative forcing due to multicomponent anthropogenic and natural aerosols. *J. Geophys. Res*. **106**, 1551–1568.

Jacobson, M. Z. 2002. Control of fossil-fuel particulate black carbon and organic matter, possibly the most effective method of slowing global warming. *J. Geophys. Res.*. **107**(D19), 4410.

Jacobson, M. Z. 2005. A solution to the problem of non-equilibrium acid/base gas-particle transfer at long time step. *Aerosol Sci. Tech*. **39**, 92–103.

Jeuken, A., Veefkind, J. P., Dentener, F., Metzger, S. and Gonzalez, C. R. 2001. Simulation of the aerosol optical depth over Europe for August 1007 and a comparison with observations. *J. Geophys. Res.*. **106**, 28295–28311.

Junker, C. and Liousse, C. 2006. A global emission inventory of carbonaceous aerosol from historic records of fossil fuel and biofuel consumption for the period 1860-1997. *Atmos. Chem. Phys. Discuss.* **6**, 4897–4927.

Kahnert, E. 2002. Measurements of particulate matter. *Status report 2002, EMEP/ CCC-Report 4*. (http://www.nilu.no/projects/CCC/onlinedata/pm/index.html)

Kulmala, M., Laaksonen, A. and Pirjola, L. 1998. Parameterizations for sulfuric acid/water nucelation rates. *J. Geophys. Res.*. **103**, 8301–8308.

Lavoue, D., Liousse, C., Cachier, H., Stocks, B. J. and Goldammer, J. G. 2000. Modeling of carbonaceous particles emitted by boreal and temperate wild-fires at northern latitudes. *J. Geophys. Res*. **105**, 26871–26890.

Lelieveld, co-authors. 2001. The Indian ocean experiment: widespread air pollution from South and Southeast Asia. *Science* **291**, 1031–1036.

Lim, H. J., Carlton, A. G. and Turpin, B. J. 2005. Isoprene forms secondary organic aerosol through cloud processing: model simulations. *Environ. Sci. Technol.* **39**, 4441–4446.

Liousse, C., Penner, J. E., Chuang, C., Walton, J. J., Eddleman, H. and co-authors. 1996. A global three-dimensional model study of carbonaceous aerosols. *J. Geophys. Res*. **105**, 26871–26890.

Liousse, C., Andreae, M. O., Artaxo, P., Barbosa, P., Cachier, H. and co-authors. 2004. Deriving global quantitative estimates for spatial and temporal distributions of biomass burning emissions. In: *Emissions of Atmospheric Trace Compounds*. (eds C. Granier, P. Artaxo and C. Reeves). Kluwer Academic Publishers, Dordrecht, The Netherlands, 544.

Liousse, C., Michel, C., Bessagnet, B., Cachier, H. and Rosset, R. 2005. 0D-modelling of carbonaceous aerosols over greater paris focusing on the organic particle formation. *J. Atmos. Chem*. **51**(2), 207–221.

Liu, X., Penner, J. E. and Herzog, M. 2005. Global modeling of aerosol dynamics: Model description, evaluation, and interactions between sulfate and nonsulfate aerosols. *J. Geophys. Res.* **110**, D18206, doi:10.1029/2004JD005674.

Lohmann, U., Feichter, J., Chuang, C. C. and Penner, J. E. 1999. Predicting the number of cloud droplets in the ECHAM-GCM. *J. Geophys. Res*. **104**, 9169–9198.

Martin-Reviejo, M. and Wirtz, K. 2005. Is benzene a precursor for secondary organic aerosol?. *Environ. Sci. Technol*. **39**, 1045–1054.

Ming, Y., Ramaswamy, V., Leo J., Donner and Phillips, V. T. J. 2006. A new parameterization of cloud droplet activation applicable to general circulation models. *J. Atmos. Sci.*. **63**(4), 1348–1356.

Nenes, A., Pandis, S. N. and Pilinis, C. 1998. ISORROPIA: a new thermodynamic equilibrium model for multiphase multicomponent inorganic aerosols. *Aqua. Geochem*. **4**, 123–152.

Nenes, A. and Seinfeld, J. H. 2003. Parametrization of cloud drop formation in global climate models. *J. Geophys. Res*. **108**, 4415. doi:10.1029/2002JD002101.

Odum, J. R., Hoffman, T., Bowman, F., Collins, D., Flagan, R. C. and co-authors. 1996. Gas-Particle partitioning and secondary aerosol yield. *Environ. Sci. Tech.* **30**, 2580–2585.

Olivier, J., Peters, J., Granier, C., Petron, G., Müller, J.-F. and co-authors. 2003. Present and future surface emissions of atmospheric compounds. *POET report #2, EU project EVK2-1999–00011*.

Olivier, J. G. J., Bouwman, A. F., Berdowski, J. J. M., Veldt, C., Bloos, J. P. J. and co-authors. 1999. Sectoral emission inventories of greenhouse gases for 1990 on a per country basis as well as on $1^\circ \times 1^\circ$ degrees. *Environ. Sci. Policy*. **2**, 241–263.

Olson, J. S., Watts, J. and Allison, L. 1983. Carbon in live vegetation of major world ecosystems. *W-7405-ENG-26, U.S. Department of Energy, Oak Ridge National Laboratory*.

Pandis, S. N., Harley, R. A., Cass, G. R. and Seinfeld, J. H. 1992. Secondary organic aerosol formation and transport. *Atmos. Environ.* **26A**, 2269–2282.

Penner, J. E., Dickinson, R. E. and O'Neill, C.A. 1992. Effects of aerosol from biomass burning on the global radiation budget. *Science*. **256**, 1432–1433.

Pilinis, C., Capaldo, K., Nenes, A. and Pandis, S. N. 2000. MADM – A new multicomponent aerosol dynamics model. *Aerosol Sci. Tech*. **32**, 482–502.

Pöschl, U., Letzel, T., Schauer, C. and Niessner, R.2001. Interaction of ozone and water vapour with spark discharge soot aerosol coated with benzo[a]pyrene: O3 and H2O adsorption, benzo[a]pyrene degradation and atmospheric implications. *J. Phys. Chem. A*. **105**, 4029–4041.

Pun, B. K., Wu, S.-Y., Seigneur, C., Seinfeld, J. H., Griffin, R. J. and co-authors. 2003. Uncertainties in modelling secondary organic aerosols : three-dimensional modelling studies on Nashville/Tennessee. *Environ. Sci. Technol*. **37**, 3647–3661.

Pun, B. K., Seigneur, C., Vijayaraghavan, K., Wu, S., Chen, S. and co-authors. 2006. Modeling regional haze in the BRAVO study using CMAQ-MADRID: 1. Model evaluation. *J. Geophys. Res.* **111**, D06302, doi:10.1029/2004JD005608.

Riemer, N., Vogel, H. and Vogel, B. 2004. Soot ageing time scales in polluted regions during day and night. *Atmos. Chem. Phys*. **4**, 1885–1893.

Rodriguez, M. A. and Dabdub, D. 2004. IMAGE-SCAPE2: A modelling study of size- and chemically resolved aerosol thermodynamics in a global chemical transport model. *J. Geophys. Res*. **109**, D02203, doi:10.1029/2003JD003639.

Russell, G. L. and Lerner, J. A. 1981. A new finite-differencing scheme for the tracer transport equations. *J. Appl. Met*. **20**, 1483–1498.

Schaap, M., GDenier Van Der on, H. A. C., Dentener, F. J., Visschedijk, A. J. H., Van Loon, M. and co-authors. 2004. Anthropogenic black carbon and fine aerosol distribution over Europe. *J. Geophys. Res.* **109**, D18207. doi:10.1029/2003JD004330.

Seinfeld, J. H. and Pandis, S. N. 1998. *Atmospheric Chemistry and Physics*. John Wiley and Sons, New York.

Slinn, W. G. N. 1977. Some approximations for the wet and dry removal of particles and gases from the atmosphere. *Water, Air, Soil Pollut.* **7**, 513–543.

Solmon, F., Giorgi, F. and Liousse, C. 2006. Development of a regional anthropogenic aerosol model for climate studies: application and validation over a European/African domain. *Tellus* **58B**, 51–72.

Spracklen, D. V., Pringle, K. J., Carslaw, K. S., Chipperfield, M. P. and Mann, G. W. 2005. A global off-line model of size-resolved aerosol microphysics: I. Model development and prediction of aerosol properties. *Atmos. Chem.. Phys. Discuss.* **5**, 179–215.

Stier, P., Feichter, J., Kinne, S., Vignati, E., Wilson, J. and co-authors. 2004. The aerosol-climate model ECHAM5-HAM.. *Atmos. Chem. Phys. Discuss.* **4**, 5551–5623.

Sundquist, H., Berge, E. and Kristjansson, J. E. 1989. Condensation and cloud parameterization studies with a mesoscale numerical prediction model. *Mon. Wea. Rev.* **117**, 1641–1657.

Tegen, I. and Lacis, A. A. 1996. Modelling the particle size distribution and its influence on the radiative properties of mineral dust aerosol. *J. Geophys. Res.* **101**, 19237–19244.

Tsigaridis, K. and Kanakidou, M. 2003. Global modelling of secondary organic aerosol in the troposphere: sensitivity analysis. *Atmos. Chem. Phys.* **3**, 1849–1869.

Van Velthoven, P. F. J. and Kelder, H. 1996. Estimates of Stratosphere-Troposphere Exchange: Sensitivity to model formulation and horizontal resolution. *J. Geophys. Res.* **101**, 1429–1434.

Vignati, E., Wilson, J. and Stier, P. 2004. M7: An efficient size-resolved aerosol microphysics module for large-scale aerosol transport models. *J. Geophys. Res*. **109**(D22202), doi:10.1029/2003JD004485.

Warren, D. R. and Seinfeld, J. H. 1985. Simulations of aerosol size-distribution evolution in systems with simultaneous nucleation, condensation and coagulation. *Aerosol Sci. Tech.* **4**, 31–43.

Wesely, M. L. and Hicks, B. B. 2000. A review of the current status of knowledge on dry deposition. *Atmos. Environ.* **34**, 2261–2282.

Wexler, A. S. and Seinfeld, J. H. 1990. The distribution of ammonium salts among a size and composition dispersed aerosol. *Atmos. Environ.* **24A**, 1231–1246.

Wexler, A. S., Lurmann, F. W. and Seinfeld, J. H. 1994. Modeling urban and regional aerosols, 1, Model development. *Atmos. Environ*. **28**, 531–546.

Zhang, Y., Pun, B., Vijayaraghavan, K. and co-authors. 2004. Development and application of the Model of Aerosol Dynamics, Reaction, Ionization, and Dissolution (MADRID). *J. Geophys. Res.* **109**(D01202), doi: 10.1029/2003JD003501.